HHS Public Access

Author manuscript

J Bone Miner Res. Author manuscript; available in PMC 2019 October 02.

Published in final edited form as:

J Bone Miner Res. 2013 December ; 28(12): 2476–2489. doi:10.1002/jbmr.1992.

Hyperactive Transforming Growth Factor-β1 Signaling Potentiates Skeletal Defects in a Neurofibromatosis Type 1 Mouse Model

Steven D Rhodes[1,2], **Xiaohua Wu**[2,3], **Yongzheng He**[2,3], **Shi Chen**[2,3], **Hao Yang**[3], **Karl W Staser**[3], **Jiapeng Wang**[2,3], **Ping Zhang**[2,3], **Chang Jiang**[4], **Hiroki Yokota**[4], **Ruizhi Dong**[3], **Xianghong Peng**[5], **Xianlin Yang**[2,3], **Sreemala Murthy**[5], **Mohamad Azhar**[2,3], **Khalid S Mohammad**[5], **Mingjiang Xu**[2,3,6], **Theresa A Guise**[5], **Feng-Chun Yang**[1,2,3]

[1]Department of Anatomy and Cell Biology, Indiana University School of Medicine, Indianapolis, IN, USA

[2]Herman B. Wells Center for Pediatric Research, Indiana University School of Medicine, Indiana University School of Medicine, Indianapolis, IN, USA

[3]Department of Pediatrics, Indiana University School of Medicine, Indianapolis, IN, USA

[4]Department of Biomedical Engineering, Indiana University-Purdue University, Indianapolis, IN, USA

[5]Endocrinology and Metabolism, Department of Internal Medicine, Indiana University School of Medicine, Indianapolis, IN, USA

[6]Department of Medical and Molecular Genetics, Indiana University School of Medicine, Indianapolis, IN, USA

Abstract

Dysregulated transforming growth factor beta (TGF-β) signaling is associated with a spectrum of osseous defects as seen in Loeys-Dietz syndrome, Marfan syndrome, and Camurati-Engelmann disease. Intriguingly, neurofibromatosis type 1 (NF1) patients exhibit many of these characteristic skeletal features, including kyphoscoliosis, osteoporosis, tibial dysplasia, and pseudarthrosis; however, the molecular mechanisms mediating these phenotypes remain unclear. Here, we provide genetic and pharmacologic evidence that hyperactive TGF-β1 signaling pivotally underpins osseous defects in *Nf1*$^{flox/-}$;*Col2.3Cre* mice, a model which closely recapitulates the skeletal abnormalities found in the human disease. Compared to controls, we show that serum TGF-β1 levels are fivefold to sixfold increased both in *Nf1*$^{flox/-}$;*Col2.3Cre* mice and in a cohort of NF1 patients. *Nf1*-deficient osteoblasts, the principal source of TGF-β1 in bone, overexpress TGF-β1

Address correspondence to: Feng-Chun Yang, MD, PhD, Indiana University School of Medicine, Cancer Research Institute, 1044 W. Walnut St., Building R4, Room 427, Indianapolis, IN 46202, USA. fyang@iupui.edu.

Additional Supporting Information may be found in the online version of this article.

Disclosures

All authors state that they have no conflicts of interest.

Authors' roles: Study design: SDR, KSM, MX, TAG, and FCY. Study conduct: SDR, XW, YH, SC, HY, KWS, JW, PZ, CJ, HY, RD, XP, XY, and SM. Data analysis and interpretation: SDR, KSM, MX, and FCY. Drafting manuscript: SDR and FCY. Revising manuscript content: SDR, KWS, MA, KSM, MX, TAG, and FCY. Approving final version of manuscript: FCY.

in a gene dosage–dependent fashion. Moreover, *Nf1*-deficient osteoblasts and osteoclasts are hyperresponsive to TGF-β1 stimulation, potentiating osteoclast bone resorptive activity while inhibiting osteoblast differentiation. These cellular phenotypes are further accompanied by p21-Ras–dependent hyperactivation of the canonical TGF-β1–Smad pathway. Reexpression of the human, full-length neurofibromin guanosine triphosphatase (GTPase)-activating protein (GAP)-related domain (*NF1* GRD) in primary *Nf1*-deficient osteoblast progenitors, attenuated TGF-β1 expression levels and reduced Smad phosphorylation in response to TGF-β1 stimulation. As an in vivo proof of principle, we demonstrate that administration of the TGF-β receptor 1 (TβRI) kinase inhibitor, SD-208, can rescue bone mass deficits and prevent tibial fracture nonunion in $Nf1^{flox/-}$;*Col2.3Cre* mice. In sum, these data demonstrate a pivotal role for hyperactive TGF-β1 signaling in the pathogenesis of NF1-associated osteoporosis and pseudarthrosis, thus implicating the TGF-β signaling pathway as a potential therapeutic target in the treatment of NF1 osseous defects that are refractory to current therapies.

Keywords

TRANSFORMING GROWTH FACTOR-BETA; TGF-β; SMAD; NEUROFIBROMATOSIS TYPE 1; FRACTURE NONUNION; OSTEOPOROSIS

Introduction

Congenital pseudarthrosis, first described by James Paget in 1891, is a rare orthopedic condition characterized by anterolateral bowing of the tibia with tapering at the defective site.[1] Fractures occur early in life, and fibrous nonunion can persist even after multiple surgeries. Refractory cases often require amputation to restore ambulation. Fifty percent to ninety percent of congenital tibial pseudarthrosis cases involve mutations in the *NF1* tumor suppressor gene,[2–5] which encodes Neurofibromin, a negative regulator of p21-Ras. Individuals with neurofibromatosis type 1 (NF1) have a propensity to develop a spectrum of osseous defects including osteoporosis,[6–11] dystrophic scoliosis,[12] increased fracture rates,[13,14] and pseudarthrosis,[15,16] which are associated with significant morbidity.

The molecular mechanisms responsible for low bone mass and recalcitrant fracture healing in NF1 patients are not clearly defined, yet deregulation of osteoclast and osteoblast function, the principal cellular drivers of bone resorption and bone formation, has been widely reported both in NF1 mouse models[17–20] as well as in osteoblasts and osteoclasts cultured ex vivo from human patients with the disease.[18,21,22] Transforming growth factor-beta1 (TGF-β1) has become increasingly recognized as a critical mediator of physiological and pathological skeletal remodeling. Recently, Tang and colleagues[23] demonstrated the critical role of TGF-β1 as a master switch regulating the spatiotemporal coupling of bone resorption and formation. Given the considerable phenotypic overlap between the characteristic skeletal manifestations of NF1 with those found in other TGF-β–associated disorders including Loeys-Dietz syndrome,[24–27] Marfan syndrome,[28–32] and Camurati-Engelmann disease,[33] we reasoned that dysregulated TGF-β signaling may also be integral to the pathogenesis of NF1 osseous defects.

To determine whether TGF-β signaling is altered in NF1, we generated *Nf1*$^{flox/-}$*;Col2.3Cre* mice, which recapitulate characteristic skeletal abnormalities found in NF1 patients, including low bone mass and tibial nonunion fracture.[34,35] Here, we report significantly increased TGF-β1 serum levels both in *Nf1*$^{flox/-}$*;Col2.3Cre* mice and in a cohort of NF1 patients. We further delineate a mechanism by which TGF-β1 is hypersecreted from *Nf1*-deficient osteoprogenitor cells and acts to preferentially enhance *Nf1*$^{+/-}$ osteoclast bone resorptive activity, while inhibiting osteoblast differentiation of *Nf1*$^{-/-}$ mesenchymal stem cells (MSCs). By reexpressing the human, full-length neurofibromin guanosine triphosphatase (GTPase)-activating protein (GAP) related domain (*NF1* GRD) in *Nf1*-deficient osteoprogenitor cells, we demonstrate that p21-Ras–dependent hyperactivation of the canonical TGF-β1–Smad pathway is associated with hyperresponsiveness to TGF-β1 signals by *Nf1*-deficient bone cells. Notably, treatment with a pharmacologic inhibitor of TGF-β receptor 1 (TβRI) kinase activity (SD-208) rescued bone mass defects and prevented tibial fracture nonunion in *Nf1*$^{flox/-}$*;Col2.3Cre* mice. Collectively, these data implicate dysregulated TGF-β1 signaling as a primary factor underlying the pathogenesis of NF1-associated osteoporosis and pseudarthrosis. Moreover, modulation of TGF-β signaling may serve as a potential therapeutic target in the treatment for NF1 osseous defects that are refractory to current modalities.

Materials and Methods

Animals

Nf1$^{+/-}$ mice[36] were obtained from Tyler Jacks of the Massachusetts Institute of Technology (Cambridge, MA, USA). *Nf1*$^{flox/flox}$ mice[37] were intercrossed with *Nf1*$^{+/-}$ and 2.3-kb α1 (I) collagen Cre (*Col2.3Cre*) mice[38] to generate *Nf1*$^{flox/-}$*;Col2.3Cre* mice.[34,35] For in vivo studies involving *Nf1*$^{flox/-}$*;Col2.3Cre*(+) mice, *Nf1*$^{flox/flox}$*;Col2.3Cre*(−) littermates were used as wild-type (WT) controls. For in vitro studies, MSCs harboring single and/or biallelic *Nf1* inactivation were cultured from littermates with the following genotypes: WT (*Nf1*$^{flox/flox}$*;PeriCre*(−)), *Nf1*$^{+/-}$ (*Nf1*$^{flox/-}$*;PeriCre*(−)), and *Nf1*$^{-/-}$ (*Nf1*$^{flox/-}$*;PeriCre*(+)). In this strain, the 3.9-kb fragment of the *Periostin* gene promoter is used to drive Cre expression in MSCs as reported.[35] All studies were conducted in accordance with Indiana University Laboratory Animal Research Center regulatory guidelines.

Serum TGF-β1 measurement and *Tgfb1* gene expression

Total serum TGF-β1 levels were quantified using a mouse TGF-β1 DuoSet ELISA Development kit (R&D Systems, Minneapolis, MN, USA) according to the manufacturer's protocol. TGF-β1 mRNA levels were measured by quantitative real-time PCR with SYBR Green reagents. Primers used for *Tgfb1* were CAGTGGCTGAAC-CAAGGA (forward) and AGCAGTGAGCGCTGAATCG (reverse) and for *Gapdh* TGCACCACCAACTGCTTAG (forward) and GGATG-CAGGGATGATGTTC (reverse).

Osteoclast culture and dentine slice assay

Fifty thousand (5×10^4) bone marrow mononuclear cells (BMMNCs) from *Nf1*$^{+/-}$ and WT mice were cultured in 96-well plates in α modified essential medium (α-MEM) supplemented with macrophage colony-stimulating factor (M-CSF; 30ng/mL), receptor

activator of NF-κB ligand (RANKL; 20 ng/mL), and TGF-β1 (1 ng/mL). After 3 days, the medium was changed to M-CSF (30 ng/mL), RANKL (60 ng/mL), and TGF-β1 (1 ng/mL) for an additional 3 days of culture. Osteoclasts were fixed and stained for tartrate-resistant acid phosphatase (TRACP).[18] Multinucleated, TRACP-positive-staining cells containing more than three nuclei were scored as mature osteoclasts. The bone resorptive capacity of osteoclasts was characterized by seeding 1×10^5 BMMNCs onto dentine slices. Following 7 days culture in the presence of M-CSF and RANKL at 37°C, 5% CO_2, dentine slices were rinsed with PBS and immersed overnight in 1 M ammonium hydroxide. After staining with a 1% crystal violet solution, the number and area of resorptive "pits" were quantified using NIH Image J Software on low-power fields (x100 magnification).

MSC culture and osteoblast differentiation

BMMNCs were cultured in MesenCult media (Stem Cell Technologies Inc., CA, USA) at 37°C, 5% CO_2.[19] MSCs of identical passage number (between passages 5 and 10) were used for experiments. For osteoblast differentiation, 5×10^4 MSCs were cultured for 7 days in 12-well plates using MesenCult media supplemented with 10^{-8} M dexamethasone, 5 mg/mL ascorbic acid 2-phosphate, and 10mM β-glycerophosphate. Alkaline phosphatase (ALP) staining was performed to assess osteoblast differentiation.[19]

Retroviral restoration of *NF1* GRD

MSCs were transduced with recombinant retrovirus constructs to achieve expression of the full-length *NF1* GRD under the transcriptional control of the murine stem cell virus promoter (MSCV) as described.[19,39] Puromycin (4 μg/mL) was used for cell selection.

Western blot analysis and gelatin zymography

Following stimulation with TGF-β1 and/or TβRI kinase inhibitor (SD-208), cells were lysed in a radioimmunoprecipitation assay (RIPA) lysis buffer containing protease and phosphatase inhibitors. Isolated proteins were fractionated using NuPAGE 4–12% Bis-Tris Gels (Invitrogen) and electrotransferred to polyvinylidene fluoride (PVDF) membranes. Callus proteins were harvested 14 days after tibial fracture using a mortar and pestle to grind the callus in proteolysis buffer. Immunoblots were performed using antibodies specific to p-Smad2 (Cell Signaling), total Smad2 (Cell Signaling), active TGF-β1 (R&D Systems), latent latency-associated peptide (LAP)-TGF-β1 (R&D Systems), β-actin (Sigma), and GAPDH (Cell Signaling). Gelatinolytic activities of murine myeloid cell-conditioned media and human serum samples were assessed using sodium dodecyl sulfate-polyacrylamide gel electrophoresis (SDS-PAGE) under nonreducing conditions.[40] Renaturation of the electrophoresed enzymes was achieved by incubation in a 0.15 M NaCl, 5 mM $CaCl_2$,0.05% NaN_3,50 mM Tris-HCl, pH 7.5 buffer at 37°C for 48 hours. Zones of lytic activity were revealed by Coomassie blue staining.

Smad dual-luciferase reporter assays

Osteoprogenitors were transfected with Smad reporter, negative, and positive control dual-luciferase constructs (Cignal Reporter Assay; Qiagen).[41] Transfected cells were stimulated with recombinant active TGF-β1 (1 ng/mL) or latent LAP-TGF-β1 (100 ng/mL) for 18

hours. Firefly and *Renilla* luciferase activities were measured on a 96-well microtiter plate luminometer (Thermo Labsystems) with LAR II and Stop&Glo reagents (Promega Dual Luciferase Assay Kit).

Tibial fracture and TβRI inhibitor treatment

Open tibial fractures were induced by a three-point method in 12-week-old *Nf1*$^{flox/-}$;*Col2.3Cre* mice under ketamine anesthesia as described.[35,42] Proper fracture position between the middle to distal 1/3 of the tibia below the fibular junction was confirmed by X-ray (pixRay-100; Bioptics, Phoenix, AZ, USA). Weekly radiography was performed to monitor fracture healing until the experimental endpoint of 4 weeks. The mice were treated with the TβRI kinase inhibitor, SD-208 (60 mg/kg/day), or vehicle control (1% methylcellulose in sterile water) by daily gavage.

Peripheral dual-energy X-ray absorptiometry and micro–computed tomography

Bone mineral density (BMD) was measured by peripheral dual-energy X-ray absorptiometry (pDXA) using a PIXImus mouse densitometer (GE Lunar II; Faxitron Corp., Wheeling, IL, USA) (n = 15/group). The region of interest (ROI) was defined as the distal femur just proximal to the growth plate (12×12 pixels). Formalin-fixed femurs were placed in the gantry of a micro–computed tomography (μCT) scanner (VivaCT 40; Scanco Medical AG, Bassersdorf, Switzerland). Images were acquired at a voxel size of 10.5 μm. The voxel of interest (VOI) comprised 100 transverse CT slices beginning 250 μm away from the femoral growth plate and extending proximally. Fractional bone volume (BV/TV) and architectural properties of trabecular reconstructions, including trabecular thickness (Tb.Th, mm), trabecular number (Tb.N, per mm), trabecular spacing (Tb.Sp, mm), and connectivity density (Conn.D, per mm^3) were calculated using standard algorithms.

Quantitative histomorphometry and immunohistochemistry

Tissues were fixed in 10% formalin for 48 hours, demineralized for 2 weeks in 10% EDTA, and embedded in paraffin for histological sectioning. BV/TV of the secondary spongiosa and osteoblast number (N.Ob/BS) normalized to the bone surface were quantified on hematoxylin and eosin (H&E)-stained sections of the distal femur at ×200 magnification using BIOQUANT OSTEO v11.2 software (BIOQUANT Image Analysis Inc., Nashville, TN, USA). Osteoclast number normalized to the bone surface (N.Oc/BS) was quantified on TRACP-stained sections at ×200 magnification. For immunohistochemical staining, sections were incubated in DeCal Retrieval Solution (Biogenex Laboratories, San Ramon, CA, USA) for 30 minutes at room temperature. Primary antibody to p-Smad2 (Cell Signaling; diluted 1:100) was applied overnight at 4°C. The Vectastain ABC kit containing biotinylated secondary antibody (diluted 1:2000) and 3,3’-diaminobenzidine (DAB) substrate kit (Vector Laboratories, Burlingame, CA, USA) were used for detection. Quantification of p-Smad2 staining in fracture calluses was performed with Aperio ImageScope v11.1.2.760 software using the Positive Pixel Count v9 algorithm under default settings.

Statistical analysis

Differences between experimental groups were determined by Student's *t* test or analysis of variance (ANOVA), followed by Newman-Keuls multiple comparison tests where appropriate. Values of $p < 0.05$ were considered significant.

Results

Nf1 regulates TGF-β1 expression in MSCs

In human disease, alterations in TGF-β signaling occur via several mechanisms, including aberrant ligand expression/activation, receptor mutations, and dysregulation of downstream effector pathways. We examined the serum TGF-β1 levels in $Nf1^{flox/-}$;*Col2.3Cre* mice, which closely recapitulate a spectrum of osseous manifestations seen in NF1 patients. Strikingly, we found that the serum level of total TGF-β1 in $Nf1^{flox/-}$;*Col2.3Cre* mice was elevated fivefold to sixfold as compared to WT controls (Fig. 1*A*). To identify the cell type responsible for TGF-β1 overproduction, we examined TGF-β1 expression at the mRNA and protein levels from WT, $Nf1^{+/-}$, and $Nf1^{-/-}$ osteoblast progenitors (MSCs), as this lineage is the principal source of TGF-β1 in bone.[43] $Nf1^{+/-}$ and $Nf1^{-/-}$ MSCs, as compared with WT cells, expressed significantly more TGF-β1 mRNA (Fig. 1*B*) and protein (Fig. 1*C*). Further corroborating neurofibromin's function as a negative regulator of TGF-β1 expression, we observed significantly increased serum TGF-β1 levels in human NF1 patients as compared to healthy controls (Fig. 1*D*). Collectively, these data imply that single or biallelic *Nf1* inactivation leads to pathological TGF-β1 overproduction in a gene dosage–dependent fashion.

Loss of *Nf1* leads to p21-Ras–dependent TGF-β1 overexpression and activation of the Smad pathway in MSCs, inhibiting osteoblast differentiation

Canonical TGF-β signaling involves the phosphorylation of Smad proteins by TβRI.[44] To examine the role of *Nf1* in regulating this pathway, we compared TGF-β1–induced activation of Smad2 in WT, $Nf1^{+/-}$, and $Nf1^{-/-}$ MSCs. We observed an increase in TGF-β1–induced Smad2 phosphorylation in $Nf1^{-/-}$ osteoprogenitors versus WT controls (Fig. 2*A*), whereas the total protein expression of Smad2 (Fig. 2*A*), TβRI and TβRII (Supplemental Fig. 1A) remained constant. We further postulate that increased basal levels of p-Smad2 in $Nf1^{+/-}$ and $Nf1^{-/-}$ MSCs, as compared to WT cultures, are likely indicative of the autocrine feedback effect of TGF-β1 hypersecreted by *Nf1*-deficient MSCs as characterized in Fig. 1.

To assess the implications of increased TGF-β1 biochemical activity on osteoblastogenesis, WT and $Nf1^{-/-}$ MSCs were cultured in osteogenic differentiation medium supplemented with TGF-β1. Expression of the osteoblast marker ALP, which is impaired at the baseline level in $Nf1^{-/-}$ osteoblasts, was further reduced by 87% in $Nf1^{-/-}$ cells as compared to just 53% in WT osteoblast cultures stimulated with TGF-β1 (Fig. 2*B*). Application of SD-208, an inhibitor of TβRI activity, was effective in attenuating Smad phosphorylation to basal levels (Supplemental Fig. 1B) and in rescuing ALP expression (Supplemental Fig. 1C). Collectively, these results corroborate neurofibromin's role as a suppressor of canonical TGF-β1 signaling in osteoblasts, whereby haploinsufficient or nullizygous *Nf1* gene

ablation enhances TGF-β1–dependent Smad phosphorylation and exacerbates intrinsic deficits in terminal osteoblast differentiation —a critical component of bone anabolism.

To further demonstrate that reductions in ALP activity induced by TGF-β1 in *Nf1*-deficient MSCs are reflective of an osteoblast differentiation defect, as opposed to other mechanisms such as an impaired proliferative response or lineage selection, we performed additional experiments to test these alternative hypotheses. Here we show that TGF-β1 significantly increases the proliferation of WT and $Nf1^{-/-}$ MSCs (Supplemental Fig. 1D), whereas proliferative responses to TGF-β1 were suppressed to below even basal levels following TβRI kinase inhibition (SD-208). These data are consistent with a number of studies illustrating the mitogenic effects of TGF-β1 on osteoprogenitors, as summarized by Janssens and colleagues.[43] To exclude lineage selection as a potential factor mediating the differential responses of WT and $Nf1^{-/-}$ MSCs to TGF-β1 stimulation, we compared the expression levels of several MSC cell-surface markers in WT versus $Nf1^{-/-}$ MSCs. Flow cytometric analysis revealed no differences in the expression pattern of CD105 and CD29 surface antigens when comparing WT and $Nf1^{-/-}$ MSCs (Supplemental Fig. 1E). Taken together, these data suggest that TGF-β1–mediated reductions in ALP activity in WT and *Nf1*-deficient osteoprogenitor cells are primarily due to osteoblast differentiation defects in response to TGF-β1, rather than alterations in lineage selection or an impaired proliferative response of MSCs/osteoblast progenitor cells following TGF-β1 stimulation.

Given neurofibromin's apparent function as a negative regulator of TGF-β1 expression and signaling, we therefore reasoned that p21-Ras hyperactivity may be associated with increased *Tgfb1* gene expression and Smad-dependent signaling in the absence of Nf1. To test this hypothesis, we transduced *Nf1*-deficient MSCs with a recombinant retrovirus encoding the full-length *NF1* GRD and a selectable marker, pac, which confers resistance to puromycin.[19] As compared to $Nf1^{-/-}$ MSCs expressing MSCV-pac alone, reconstitution of the full length of *NF1* GRD in *Nf1*-deficient MSCs attenuated the expression of TGF-β1 mRNA transcripts by nearly 50% (Fig. 2C) and suppressed Smad phosphorylation (Fig. 2D) following TGF-β1 stimulation. When we repeated these studies in WT MSCs, no significant differences in *Tgfb1* gene expression (Supplemental Fig. 2A) or Smad-dependent signaling (Supplemental Fig. 2B) were observed when comparing cells transduced with either the MSCV-pac or MSCV-*NF1* GRD-pac constructs. Unlike in $Nf1^{-/-}$ MSCs in which Ras activation proceeds unabated, Ras activity in WT cells is tightly regulated by endogenous full-length neurofibromin. This might explain the minimal effect on TGF-β1 expression and Smad signaling when *NF1* GRD is overexpressed in WT cells. The reduction in TGF-β1 expression and signaling specifically in *Nf1*-deficient MSCs is consistent with the normalization of Ras GTP activity following reconstitution with functional *NF1* GRD, as we have reported.[19] Collectively, these data suggest that functional inactivation of neurofibromin and p21-Ras hyperactivity are associated with dysregulation of TGF-β1 expression and Smad-dependent signaling in *Nf1*-deficient MSCs.

Hyperactive TGF-β1 signaling potentiates $Nf1^{+/-}$ osteoclast catabolic activity

Given that TGF-β1 has a pivotal impact on cellular functions of both osteoblasts and osteoclasts in bone development, we next examined the effects of TGF-β1 on aberrant bone

catabolic activity by *Nf1* haploinsufficient osteoclasts. BMMNCs cultured from $Nf1^{+/-}$ mice demonstrated a significantly increased capacity to form TRACP-positive staining, multinucleated osteoclasts following treatment with TGF-β1 as compared to WT controls (Fig. 3*A*). Application of TβRI kinase inhibitor (SD-208) attenuated osteoclast formation in a dose-dependent fashion, with an observable effect beginning at 100 nM in the $Nf1^{+/-}$ cultures as compared to 500 nM in the WT cells (Fig. 3*B*). Actin ring formation, a prerequisite for osteoclast bone resorption, was also increased in $Nf1^{+/-}$ osteoclasts cultured in the presence of TGF-β1, and suppressed by escalating concentrations of SD-208 (Supplemental Fig. 3A). To directly assess the effects of TGF-β1 on osteoclast function, WT and $Nf1^{+/-}$ osteoclasts were cultured on dentine slices in the presence of TGF-β1. $Nf1^{+/-}$ osteoclasts generated markedly increased numbers of resorptive "pits" following treatment with TGF-β1 as compared to WT controls (Fig. 3C), suggesting that TGF-β1 can preferentially activate osteoclast bone resorptive activity in the context of *Nf1* haploinsufficiency. TβRI kinase inhibition attenuated "pit" formation to basal levels in both WT and $Nf1^{+/-}$ osteoclast cultures. We further show that $Nf1^{+/-}$ osteoclast hyperresponsiveness to TGF-β1 is correlated with increased biochemical activation of the TGF-β1/Smad pathway. Increased levels of phosphorylated Smad2 were detected in $Nf1^{+/-}$ osteoclasts stimulated with TGF-β1, whereas total levels of Smad2 protein were equivalent between the two genotypes (Fig. 3*D*). Osteoclasts cultured from the peripheral blood of a human NF1 patient and an age/sex-matched healthy control exhibited a similar phenotype when treated with TGF-β1 (Supplemental Fig. 3B). In sum, these data indicate that neurofibromin functions to negatively regulate Smad-dependent TGF-β1 signaling in osteoclasts, whereby *Nf1* haploinsufficiency promotes excess osteoclast bone lytic activity via hypersensitivity to TGF-β1 stimulation.

Although $Nf1^{+/-}$ mice do not exhibit spontaneous bone mass deficits, we have previously demonstrated that they exhibit significantly increased osteolytic activity (twofold increased bone loss as compared to WT controls) in response to ovariectomy (OVX) induced pro-resorptive stress.[18] To further assess the functional contribution of hyperactive TGF-β1 signaling toward accelerated osteolytic activity in ovariectomized $Nf1^{+/-}$ mice, we tested whether TβRI kinase inhibition could abrogate excess osteoclast catabolic activity in $Nf1^{+/-}$ OVX mice. WT and $Nf1^{+/-}$ mice underwent either OVX or sham surgery followed by 6 weeks treatment with SD-208, 60 mg/kg/d, versus vehicle control (1% methylcellulose in sterile water). Here, we show that pharmacologic TβRI kinase inhibition effectively preserved femoral BMD (Supplemental Fig. 4A) and trabecular BV/TV (Supplemental Fig. 4B,C) in OVX mice as compared to the vehicle-treated cohort, in which bone loss was approximately twofold greater in the $Nf1^{+/-}$ OVX mice versus WT OVX controls. Trabecular microarchitecture parameters (Supplemental Fig. 4D–G) including Conn.D, Tb.N, Tb.Sp, and structure model index (SMI) were also restored to the level of sham-operated controls following SD-208 administration in OVX mice.

Histological methods corroborated these results (Supplemental Fig. 4H) and provided insights regarding the cellular mechanism of the observed phenotype. Osteoclast numbers, which were markedly increased in vehicle-treated $Nf1^{+/-}$ OVX mice, returned to baseline levels following SD-208 treatment (Supplemental Fig. 4I). Serum levels of the C-terminal cross-linking telopeptide of type I collagen (CTX), an established biomarker of osteolytic

activity, were significantly increased in vehicle-treated *Nf1*$^{+/-}$ OVX mice, but normalized after SD-208 treatment (Supplemental Fig. 4J). Overall, the accentuated response of *Nf1*$^{+/-}$ OVX mice to TβRI kinase inhibition underscores the pivotal role of TGF-β in potentiating osteoclast bone erosive activity in the context of *Nf1* haploinsufficiency.

TβRI inhibition rescues bone defects in *Nf1*$^{flox/-}$;*Col2.3Cre* mice

Recently, our laboratory established that *Nf1*$^{flox/-}$;*Col2.3Cre* mice spontaneously recapitulate characteristic skeletal manifestations found in NF1 patients, including low bone mass and tibial nonunion fracture.[34,35] In this model, we demonstrate that the cooperative interaction between conditional *Nf1*$^{-/-}$ osteoblasts and *Nf1*$^{+/-}$ hematopoietic cells, including osteoclasts, is integral to the pathogenesis of the bone defects.[35] Recent clinical data support this hypothesis, confirming that at least a subset of NF1 pseudarthrosis patients exhibit biallelic *NF1* inactivation in tissue microdissected from the lesion site.[45,46] Based on these findings, we reasoned that a cycle of uncoupled bone remodeling perpetuated by TGF-β1 overproduction and hypersensitivity may pivotally underlie the pathogenesis of bone defects observed in the *Nf1*$^{flox/-}$;*Col2.3Cre* murine model. Therefore, we tested whether pharmacologic inhibition of TβRI kinase activity could rescue characteristic NF1-associated bone defects such as osteoporosis and tibial fracture nonunion observed in *Nf1*$^{flox/-}$;*Col2.3Cre* mice.[34,35]

Cohorts of 3-month-old to 4-month-old *Nf1*$^{flox/-}$;*Col2.3Cre* mice received daily treatment with the TβRI kinase inhibitor, SD-208 (60 mg/kg/d) or the vehicle control (1% methylcellulose in sterile water) for 4 weeks. BMD measurements were acquired both pretreatment and posttreatment to track the percent change in BMD during the treatment period (Fig. 4*A*). μCT (Fig. 4B) and histological sections (Fig. 4C; Supplemental Fig. 5A) of the excised bones illustrate the low bone mass phenotype of vehicle treated *Nf1*$^{flox/-}$;*Col2.3Cre* mice as compared to WT controls. In contrast, dramatic increases in BMD and trabecular BV/TV (Fig. 4*A*) were observed in *Nf1*$^{flox/-}$;*Col2.3Cre* mice treated with SD-208. Although WT mice began treatment with nearly twice the bone mass of *Nf1*$^{flox/-}$;*Col2.3Cre* mice prior to therapy, we observed no significant differences in bone mass (Fig. 4*A*) or trabecular architecture parameters (Supplemental Fig. 5B–D) between WT and *Nf1*$^{flox/-}$;*Col2.3Cre* mice following SD-208 treatment, indicating that pharmacologic TGF-β inhibition completely rescued bone mass defects in the *Nf1*$^{flox/-}$;*Col2.3Cre* mice. On the cellular level, osteoblast numbers, which were diminished in vehicle-treated *Nf1*$^{flox/-}$;*Col2.3Cre* mice, were significantly increased following SD-208 treatment (Fig. 4D). By contrast, osteoclast numbers, which were elevated in vehicle-treated *Nf1*$^{flox/-}$;*Col2.3Cre* mice, were attenuated to WT levels following SD-208 treatment (Supplemental Fig. 6A,B). In summary, the striking response of *Nf1*$^{flox/-}$;*Col2.3Cre* mice to TβRI kinase inhibition—even as compared to WT animals that also received SD-208 treatment—substantiates the pivotal role of aberrant TGF-β signaling in the pathogenesis of NF1-associated osteopenia and osteoporosis in the murine system.

Nonunion fracture of long bones, particularly the tibia, carries significant morbidity in NF1 patients. This clinical feature is also recapitulated in *Nf1*$^{flox/-}$;*Col2.3Cre* mice.[35] Immunohistochemical analysis of *Nf1*$^{flox/-}$;*Col2.3Cre* mice with tibial fracture nonunion

revealed approximately threefold-increased levels of pSmad-2 within the fracture site as compared to WT controls (Fig. 5*A*). If aberrant TGF-β signaling indeed underlies recalcitrant bone healing in NF1, we reasoned that pharmacologic TβRI blockade might prevent tibial fracture nonunion in *Nf1*$^{flox/-}$*;Col2.3Cre* mice. To test this hypothesis, cohorts of *Nf1*$^{flox/-}$*;Col2.3Cre* mice were treated with SD-208 (60 mg/kg/d) or vehicle control for 6 weeks following tibial fracture. Compared to healthy WT mice, which exhibit robust callus formation, radiographic monitoring (Supplemental Fig. 7) demonstrated persistent fracture nonunion in *Nf1*$^{flox/-}$*;Col2.3Cre* mice treated with the vehicle control, with minimal or complete absence of callus formation at the fracture site. Administration of SD-208 in *Nf1*$^{flox/-}$*;Col2.3Cre* mice substantially enhanced callus formation as compared to those receiving vehicle treatment. μCT evaluation of callus structural integrity further revealed a significant increase in callus BV/TV in *Nf1*$^{flox/-}$*;Col2.3Cre* mice undergoing SD-208 treatment (Fig. 5*B*), suggesting that pharmacologic TβRI inhibition improved bone formation within the fracture site. Histological sectioning (Fig. 5C) revealed fibrous tissue and an increased presence of TRACP-positive–staining osteoclasts within the fracture site of *Nf1*$^{flox/-}$*;Col2.3Cre* mice receiving vehicle treatment. SD-208 treatment significantly reduced osteoclast numbers and p-Smad2 levels (Fig. 5*D*) within the fracture callus. Collectively, these results provide the first direct evidence that pharmacologic TGF-β blockade is an effective therapeutic strategy to augment bone healing in a mouse model of NF1 tibial pseudarthrosis.

Hypersecretion of matrix metalloproteinase-2 or matrix metalloproteinase-9 potentiates latent TGF-β1 activation

In order for TGF-β1 to bind to its receptors and exert its biological effects, it must be cleaved from its LAP. When we measured the levels of latent, LAP-bound TGF-β1 versus active TGF-β1 in *Nf1*$^{flox/-}$*;Col2.3Cre* mice with tibial fracture nonunion, we observed a dramatic increase in the ratio of active-to-latent TGF-β1 within the facture site as compared to WT controls (Fig. 6*A*), implying that accelerated conversion of latent TGF-β1 to the active form may play an important role in upregulating the bioavailability of active TGF-β1. Cleavage of the TGF-β LAP is known to occur through both acid and enzymatic mechanisms.[47] Among these, matrix metalloproteinase 2 (MMP-2) and MPP-9 have been shown to mediate the proteolysis of LAP and play an important role in bone remodeling and fracture healing in animal models.[48–51] We next measured the levels of active MMPs in the conditioned medium of *Nf1* haploinsufficient myeloid cells by gelatin zymography. In particular, the gelatinase activity of MMP-2/9 was significantly enhanced in *Nf1*$^{+/-}$ myeloid cell conditioned medium versus WT controls (Fig. 6B; Supplemental Fig. 8A). We similarly observed a 5.4-fold increase in MMP-2 activity in the serum of a NF1 patient as compared to a matched, healthy control (Supplemental Fig. 8B,C). To demonstrate that only the active form of TGF-β1 can promote hyperactivation of the canonical Smad pathway, we transfected *Nf1* nullizygous osteoprogenitors with a Smad luciferase reporter construct and subsequently stimulated the transfected cells with either recombinant, active TGF-β1 (1 ng/mL) or 100 times the dose of latent, LAP-bound TGF-β1 (100 ng/mL). Expectedly, Smad luciferase reporter activity was nearly 75% greater in *Nf1*$^{-/-}$ osteoprogenitors stimulated with recombinant active TGF-β1 as compared to WT controls, but not in cells stimulated with LAP-TGF-β1 (Fig. 6*C*).

Discussion

The precise role of TGF-β1 in regulating skeletal homeostasis has been historically difficult to define. Observations that exogenously administered TGF-β1 can stimulate bone formation[14,40,52] implicate TGF-β1 as an anabolic factor in bone metabolism. Conversely, recent genetic[53,54] and pharmacologic[55,56] data demonstrate that attenuation of endogenous TGF-β1 signaling may in fact augment bone mass and quality by simultaneously enhancing osteoblast differentiation while inhibiting osteoclast recruitment. Here, we demonstrate that hyperactive TGF-β1 signaling plays a pivotal role in the pathogenesis of fracture nonunion and osteoporosis in a mouse model of the common autosomal dominant genetic disorder, NF1.

Previous genetic studies suggest that either overabundance or deficiency of TGF-β1 can lead to poor bone quality. TGF-β1 knockout mice exhibit reduced BMD, cortical thickness, and fracture toughness.[57,58] By contrast, mice overexpressing TGF-β in osteoblasts show gene dosage–dependent reductions in bone mineral concentration, elastic modulus, and hardness.[54] Tang and colleagues[23] recently established a murine model that carries a Camurati-Engelmann disease (CED)-derived mutant TGF-β1. These TGF-β1 mutant mice demonstrate high levels of active TGF-β1 and exhibit progressive diaphyseal dysplasia similar to that seen in patients with CED.[23] Similarly, individuals with Loeys-Dietz and Marfan syndrome, both of which involve altered TGF-β signaling, exhibit characteristic skeletal manifestations including osteopenia,[25,26,29–31] scoliosis,[24,32,59] and an increased incidence of pseudarthrosis following orthopedic instrumentation.[60,61] It has been hypothesized that chronically elevated serum TGF-β levels may also underlie bone loss in states such as hepatic and/or renal osteodystrophy.[62]

In the present study, we show that *Nf1*$^{flox/-}$*;Col2.3Cre* mice, which recapitulate multiple NF1-associated skeletal abnormalities including osteoporosis and nonunion fracture healing,[34,35] exhibit fivefold to sixfold elevated serum TGF-β1 levels as compared to WT controls. Serum TGF-β1 levels were similarly increased in a cohort of human NF1 patients, as shown herein. Consistent with these data, we previously reported that *Nf1* haploinsufficient mast cells hypersecrete TGF-β, perpetuating excessive fibroblast proliferation and collagen synthesis within the neurofibroma microenvironment.[63] More recently, Wang and colleagues[64] noted increased TGF-β mRNA levels in the fracture calluses of mice harboring conditional *Nf1* nullizygous osteoblasts.

Beyond merely overexpressing TGF-β1, *Nf1* mutant osteoblasts and osteoclasts pathologically differentiated and excessively resorbed bone in response to TGF-β1. These cellular dysfunctions were associated with increased activation of the canonical Smad pathway. Reexpression of the human, full-length *NF1* GRD in *Nf1*-deficient osteoprogenitors attenuated TGF-β1 expression levels and inhibited Smad phosphorylation in response to TGF-β1 stimulation, thus validating that TGF-β1–mediated biochemical gain-in-functions within neurofibromin-deficient bone cells occur in a p21-Ras–dependent fashion.

The elevated ratio of active-to-latent TGF-β1 in *Nf1*$^{flox/-}$;*Col2.3Cre* mice with tibial fracture nonunion further suggests that accelerated cleavage of the TGF-β1 LAP may also play an important role in upregulating the bioavailability of active TGF-β1 within the bone matrix. Several factors are known to activate latent TGF-β, including integrins,[65] thrombospondin-1,[66] and MMP-2/9.[67] In the present study, we found increased levels of active MMP-2 and MMP-9 in both the conditioned media of *Nf1* haploinsufficient myeloid cells and the serum of a human NF1 patient as compared to controls. Intriguingly, genetic ablation of MMP-2 and MMP-9 has been shown to alter bone remodeling[51] and fracture repair.[48,50] Moreover, patient-derived hypertrophic nonunion fracture tissue was also found to overexpress MMP-7 and MMP-12 in a recent clinical study.[49] Collectively, these findings suggest the need for further investigation regarding the relationship between MMPs and TGF-β1 activation in normal and *Nf1*-deficient bone healing.

Recent clinical studies[21,22,45] and animal models[18,34,35,64,68–70] suggest that cooperative interactions between local *Nf1*-nullizygous osteoprogenitors and *Nf1* haploinsufficient osteoclasts of the bone marrow play a critical role in modulating the disease process. By restoring the balance of coordinated osteoclast and osteoblast activity in NF1, attenuating TGF-β signaling may hold advantages over traditional monotherapies such as bisphosphonates, parathyroid hormone (PTH), bone morphogenic protein (BMP), or vitamin D, which selectively target either the osteoclast or the osteoblast alone. Furthermore, Heervä and colleagues[71] recently demonstrated that osteoclasts derived from human NF1 patients were insensitive to bisphosphonate treatment versus healthy controls, reinforcing the need to develop novel targeted therapies designed specifically for the NF1 patient population. Here, we show that suppression of hyperactive TGF-β signaling can normalize the dysregulated functioning of *Nf1*-deficient osteoblasts and osteoclasts, thereby restoring bone mass and preventing tibial fracture nonunion in *Nf1*$^{flox/-}$;*Col2.3Cre* mice. These results underscore the need for next-generation, highly selective TGF-β pharmacological inhibitors that could effectively treat the current therapy-resistant bone pathologies of NF1 patients.

In summary, this study provides direct preclinical evidence that dysregulated TGF-β signaling underlies osteoporosis and nonunion fracture in patients with NF1. These in vivo data also verify the regulatory role of TGF-β signaling in osteoclast and osteoblast biology —a complex topic that has been historically difficult to assess as a result of biphasic and dose-dependent effects of TGF-β on bone cells in in vitro culture. The marked response of *Nf1*$^{flox/-}$;*Col2.3Cre* mice to pharmacologic TGF-β inhibition—even as compared to WT controls also undergoing treatment—underscores the critical importance of the TGF-β pathway in the genesis of NF1-associated bone defects and as a target for therapeutic intervention. Taken together, these data suggest a proposed model (Fig. 6D) in which genetic inactivation of *Nf1* in osteoprogenitor cells results in increased TGF-β1 synthesis and systemically elevated TGF-β1 levels. We further postulate that excess quantities of latent, LAP-bound TGF-β1 sequestered within the bone matrix may be liberated at an accelerated rate by hyperresorptive *Nf1*$^{+/-}$ osteoclasts and subsequently activated by increased levels of MMP-2 and MMP-9 secreted by *Nf1* haploinsufficient myeloid cells. In turn, we propose that active TGF-β1 feeds back to perpetuate a cycle of accelerated osteolytic activity while simultaneously suppressing a compensatory osteoblast anabolic response. At the molecular level, hypersensitivity of *Nf1*-deficient bone cells to TGF-β1 stimulation was associated

with increased biochemical activation of the Smad pathway. Further supporting the paradigm that aberrant TGF-β1 signaling pivotally underpins NF1-associated osseous defects, we demonstrate that disruption of this pathological paracrine circuitry via pharmacologic inhibition of TβRI kinase activity (SD-208) can rescue bone mass deficits and prevent tibial fracture nonunion in *Nf1*$^{flox/-}$*;Col2.3Cre* mice. Given that current treatment outcomes for pseudarthrosis in NF1 remain poor, the potential application of pharmacologic TGF-β inhibitors to augment bone union warrants further preclinical and early phase clinical trials.

Acknowledgments

This research was supported by the U.S. Department of Defense (DOD) (NF043032 to FCY; NF073112 to FCY; March of Dimes (YF08-246 to FCY); Children's Tumor Foundation (2011-01-010 to SDR); and Indiana Clinical and Translational Sciences Institute PHS NCCR (5TL1RR025759-03 to SDR).

References

1. Peltier LF. The classic. Ununited fractures in children. James Paget, 1891. Clin Orthop Relat Res. 1982 Jun.(166):2–4.
2. Sofield HA. Congenital pseudarthrosis of the tibia. Clin Orthop Relat Res. 1971 May.76:33–42. [PubMed: 4996080]
3. Morrissy RT, Riseborough EJ, Hall JE. Congenital pseudarthrosis of the tibia. J Bone Joint Surg Br. 1981; 63-B(3):367–375. [PubMed: 6790551]
4. Gilbert A, Brockman R. Congenital pseudarthrosis of the tibia. Long-term followup of 29 cases treated by microvascular bone transfer. Clin Orthop Relat Res. 1995 May.(314):37–44.
5. Ippolito E, Corsi A, Grill F, Wientroub S, Bianco P. Pathology of bone lesions associated with congenital pseudarthrosis of the leg. J Pediatr Orthop B. 2000 Jan; 9(1):3–10. [PubMed: 10647102]
6. Dulai S, Briody J, Schindeler A, North KN, Cowell CT, Little DG. Decreased bone mineral density in neurofibromatosis type 1: results from a pediatric cohort. J Pediatr Orthop. 2007 Jun; 27(4):472–475. [PubMed: 17513973]
7. Stevenson DA, Moyer-Mileur LJ, Murray M, Slater H, Sheng X, Carey JC, Dube B, Viskochil DH. Bone mineral density in children and adolescents with neurofibromatosis type 1. J Pediatr. 2007 Jan; 150(1):83–88. [PubMed: 17188620]
8. Yilmaz K, Ozmen M, Bora Goksan S, Eskiyurt N. Bone mineral density in children with neurofibromatosis 1. Acta Paediatr. 2007 Aug; 96(8):1220–1222. [PubMed: 17608828]
9. Illes T, Halmai V, de Jonge T, Dubousset J. Decreased bone mineral density in neurofibromatosis-1 patients with spinal deformities. Osteoporos Int. 2001; 12(10):823–827. [PubMed: 11716184]
10. Kuorilehto T, Poyhonen M, Bloigu R, Heikkinen J, Vaananen K, Peltonen J. Decreased bone mineral density and content in neurofibromatosis type 1: lowest local values are located in the load-carrying parts of the body. Osteoporos Int. 2005 Aug; 16(8):928–936. [PubMed: 15551055]
11. Lammert M, Kappler M, Mautner VF, Lammert K, Storkel S, Friedman JM, Atkins D. Decreased bone mineral density in patients with neurofibromatosis 1. Osteoporos Int. 2005 Sep; 16(9):1161–1166. [PubMed: 15988556]
12. Vitale MG, Guha A, Skaggs DL. Orthopaedic manifestations of neurofibromatosis in children: an update. Clin Orthop Relat Res. 2002 Aug.(401):107–118.
13. Tucker T, Schnabel C, Hartmann M, Friedrich RE, Frieling I, Kruse HP, Mautner VF, Friedman JM. Bone health and fracture rate in individuals with neurofibromatosis 1 (NF1). J Med Genet. 2009 Apr; 46(4):259–265. [PubMed: 19066167]
14. Heerva E, Koffert A, Jokinen E, Kuorilehto T, Peltonen S, Aro HT, Peltonen J. A controlled register-based study of 460 neurofibroma-tosis 1 patients: increased fracture risk in children and adults over 41 years of age. J Bone Miner Res. 2012 Nov; 27(11):2333–2337. [PubMed: 22692994]

15. Friedman JM, Birch PH. Type 1 neurofibromatosis: a descriptive analysis of the disorder in 1,728 patients. Am J Med Genet. 1997 May 16; 70(2):138–143. [PubMed: 9128932]
16. Stevenson DA, Birch PH, Friedman JM, Viskochil DH, Balestrazzi P, Boni S, Buske A, Korf BR, Niimura M, Pivnick EK, Schorry EK, Short MP, Tenconi R, Tonsgard JH, Carey JC. Descriptive analysis of tibial pseudarthrosis in patients with neurofibromatosis 1. Am J Med Genet. 1999 Jun 11; 84(5):413–419. [PubMed: 10360395]
17. Yu X, Chen S, Potter OL, Murthy SM, Li J, Pulcini JM, Ohashi N, Winata T, Everett ET, Ingram D, Clapp WD, Hock JM. Neurofibromin and its inactivation of Ras are prerequisites for osteoblast functioning. Bone. 2005 May; 36(5):793–802. [PubMed: 15804420]
18. Yang FC, Chen S, Robling AG, Yu X, Nebesio TD, Yan J, Morgan T, Li X, Yuan J, Hock J, Ingram DA, Clapp DW. Hyperactivation of p21ras and PI3K cooperate to alter murine and human neurofibromatosis type 1-haploinsufficient osteoclast functions. J Clin Invest. 2006 Nov; 116(11): 2880–2891. [PubMed: 17053831]
19. Wu X, Estwick SA, Chen S, Yu M, Ming W, Nebesio TD, Li Y, Yuan J, Kapur R, Ingram D, Yoder MC, Yang FC. Neurofibromin plays a critical role in modulating osteoblast differentiation of mesenchymal stem/progenitor cells. Hum Mol Genet. 2006 Oct 1; 15(19):2837–2845. [PubMed: 16893911]
20. Elefteriou F, Benson MD, Sowa H, Starbuck M, Liu X, Ron D, Parada LF, Karsenty G. ATF4 mediation of NF1 functions in osteoblast reveals a nutritional basis for congenital skeletal dysplasiae. Cell Metab. 2006 Dec; 4(6):441–451. [PubMed: 17141628]
21. Heerva E, Alanne MH, Peltonen S, Kuorilehto T, Hentunen T, Vaananen K, Peltonen J. Osteoclasts in neurofibromatosis type 1 display enhanced resorption capacity, aberrant morphology, and resistance to serum deprivation. Bone. 2010 Sep; 47(3):583–590. [PubMed: 20541045]
22. Stevenson DA, Yan J, He Y, Li H, Liu Y, Zhang Q, Jing Y, Guo Z, Zhang W, Yang D, Wu X, Hanson H, Li X, Staser K, Viskochil DH, Carey JC, Chen S, Miller L, Roberson K, Moyer-Mileur L, Yu M, Schwarz EL, Pasquali M, Yang FC. Multiple increased osteoclast functions in individuals with neurofibromatosis type 1. Am J Med Genet A. 2011 May; 155A(5):1050–1059. [PubMed: 21465658]
23. Tang Y, Wu X, Lei W, Pang L, Wan C, Shi Z, Zhao L, Nagy TR, Peng X, Hu J, Feng X, Van Hul W, Wan M, Cao X. TGF-beta1-induced migration of bone mesenchymal stem cells couples bone resorption with formation. Nat Med. 2009 Jul; 15(7):757–765. [PubMed: 19584867]
24. Loeys BL, Chen J, Neptune ER, Judge DP, Podowski M, Holm T, Meyers J, Leitch CC, Katsanis N, Sharifi N, Xu FL, Myers LA, Spevak PJ, Cameron DE, De Backer J, Hellemans J, Chen Y, Davis EC, Webb CL, Kress W, Coucke P, Rifkin DB, De Paepe AM, Dietz HC. A syndrome of altered cardiovascular, craniofacial, neurocognitive and skeletal development caused by mutations in TGFBR1 or TGFBR2. Nat Genet. 2005 Mar; 37(3):275–281. [PubMed: 15731757]
25. Kirmani S, Tebben PJ, Lteif AN, Gordon D, Clarke BL, Hefferan TE, Yaszemski MJ, McGrann PS, Lindor NM, Ellison JW. Germline TGF-beta receptor mutations and skeletal fragility: a report on two patients with Loeys-Dietz syndrome. Am J Med Genet A. 2010 Apr; 152A(4):1016–1019. [PubMed: 20358619]
26. Ben Amor IM, Edouard T, Glorieux FH, Chabot G, Tischkowitz M, Roschger P, Klaushofer K, Rauch F. Low bone mass and high material bone density in two patients with Loeys-Dietz syndrome caused by transforming growth factor receptor 2 mutations. J Bone Miner Res. 2012 Mar; 27(3):713–718. [PubMed: 22095581]
27. Sousa SB, Lambot-Juhan K, Rio M, Baujat G, Topouchian V, Hanna N, Le Merrer M, Brunelle F, Munnich A, Boileau C, Cormier-Daire V. Expanding the skeletal phenotype of Loeys-Dietz syndrome. Am J Med Genet A. 2011 May; 155A(5):1178–1183. [PubMed: 21484991]
28. Wilner HI, Finby N. Skeletal Manifestations in the Marfan syndrome. JAMA. 1964 Feb 15.187:490–495. [PubMed: 14084820]
29. Kohlmeier L, Gasner C, Bachrach LK, Marcus R. The bone mineral status of patients with Marfan syndrome. J Bone Miner Res. 1995 Oct; 10(10):1550–1555. [PubMed: 8686512]
30. Le Parc JM, Plantin P, Jondeau G, Goldschild M, Albert M, Boileau C. Bone mineral density in sixty adult patients with Marfan syndrome. Osteoporos Int. 1999; 10(6):475–479. [PubMed: 10663348]

31. Moura B, Tubach F, Sulpice M, Boileau C, Jondeau G, Muti C, Chevallier B, Ounnoughene Y, Le Parc JM. Bone mineral density in Marfan syndrome A large case-control study. Joint Bone Spine. 2006 Dec; 73(6):733–735. [PubMed: 17056292]
32. Demetracopoulos CA, Sponseller PD. Spinal deformities in Marfan syndrome. Orthop Clin North Am. 2007 Oct; 38(4):563–572. [PubMed: 17945136]
33. Janssens K, Vanhoenacker F, Bonduelle M, Verbruggen L, Van Maldergem L, Ralston S, Guanabens N, Migone N, Wientroub S, Divizia MT, Bergmann C, Bennett C, Simsek S, Melancon S, Cundy T, Van Hul W. Camurati-Engelmann disease: review of the clinical, radiological, and molecular data of 24 families and implications for diagnosis and treatment. J Med Genet. 2006 Jan; 43(1):1–11. [PubMed: 15894597]
34. Zhang W, Rhodes SD, Zhao L, He Y, Zhang Y, Shen Y, Yang D, Wu X, Li X, Yang X, Park SJ, Chen S, Turner C, Yang FC. Primary osteopathy of vertebrae in a neurofibromatosis type 1 murine model. Bone. 2011 Jun 1; 48(6):1378–1387. [PubMed: 21439418]
35. Wu X, Chen S, He Y, Rhodes SD, Mohammad KS, Li X, Yang X, Jiang L, Nalepa G, Snider P, Robling AG, Clapp DW, Conway SJ, Guise TA, Yang FC. The haploinsufficient hematopoietic microenvironment is critical to the pathological fracture repair in murine models of neurofibromatosis type 1. PLoS One. 2011; 6(9):e24917. [PubMed: 21980365]
36. Jacks T, Shih TS, Schmitt EM, Bronson RT, Bernards A, Weinberg RA. Tumour predisposition in mice heterozygous for a targeted mutation in Nf1. Nat Genet. 1994 Jul; 7(3):353–361. [PubMed: 7920653]
37. Zhu Y, Romero MI, Ghosh P, Ye Z, Charnay P, Rushing EJ, Marth JD, Parada LF. Ablation of NF1 function in neurons induces abnormal development of cerebral cortex and reactive gliosis in the brain. Genes Dev. 2001 Apr 1; 15(7):859–876. [PubMed: 11297510]
38. Dacquin R, Starbuck M, Schinke T, Karsenty G. Mouse alpha1(I)-collagen promoter is the best known promoter to drive efficient Cre recombinase expression in osteoblast. Dev Dyn. 2002 Jun; 224(2):245–251. [PubMed: 12112477]
39. Hiatt KK, Ingram DA, Zhang Y, Bollag G, Clapp DW. Neurofibromin GTPase-activating protein-related domains restore normal growth in Nf1−/− cells. J Biol Chem. 2001 Mar 9; 276(10):7240–7245. [PubMed: 11080503]
40. Xu M, Bruno E, Chao J, Huang S, Finazzi G, Fruchtman SM, Popat U, Prchal JT, Barosi G, Hoffman R. Constitutive mobilization of CD34þ cells into the peripheral blood in idiopathic myelofibrosis may be due to the action of a number of proteases. Blood. 2005 Jun 1; 105(11): 4508–4515. [PubMed: 15705794]
41. Pollari S, Leivonen SK, Perala M, Fey V, Kakonen SM, Kallioniemi O. Identification of microRNAs inhibiting TGF-beta-induced IL-11 production in bone metastatic breast cancer cells. PLoS One. 2012; 7(5):e37361. [PubMed: 22629385]
42. Bonnarens F, Einhorn TA. Production of a standard closed fracture in laboratory animal bone. J Orthop Res. 1984; 2(1):97–101. [PubMed: 6491805]
43. Janssens K, ten Dijke P, Janssens S, Van Hul W. Transforming growth factor-beta1 to the bone. Endocr Rev. 2005 Oct; 26(6):743–774. [PubMed: 15901668]
44. Derynck R, Zhang YE. Smad-dependent and Smad-independent pathways in TGF-beta family signalling. Nature. 2003 Oct 9; 425(6958):577–584. [PubMed: 14534577]
45. Stevenson DA, Zhou H, Ashrafi S, Messiaen LM, Carey JC, D'Astous JL, Santora SD, Viskochil DH. Double inactivation of NF1 in tibial pseudarthrosis. Am J Hum Genet. 2006 Jul; 79(1):143–148. [PubMed: 16773574]
46. Lee SM, Choi IH, Lee DY, Lee HR, Park MS, Yoo WJ, Chung CY, Cho TJ. Is double inactivation of the Nf1 gene responsible for the development of congenital pseudarthrosis of the tibia associated with NF1? J Orthop Res. 2012 Oct; 30(10):1535–1540. [PubMed: 22488919]
47. Annes JP, Munger JS, Rifkin DB. Making sense of latent TGFbeta activation. J Cell Sci. 2003 Jan 15; 116(Pt 2):217–224. [PubMed: 12482908]
48. Colnot C, Thompson Z, Miclau T, Werb Z, Helms JA. Altered fracture repair in the absence of MMP9. Development. 2003 Sep; 130(17):4123–4133. [PubMed: 12874132]

49. Fajardo M, Liu CJ, Ilalov K, Egol KA. Matrix metalloproteinases that associate with and cleave bone morphogenetic protein-2 in vitro are elevated in hypertrophic fracture nonunion tissue. J Orthop Trauma. 2010 Sep; 24(9):557–563. [PubMed: 20736794]
50. Lieu S, Hansen E, Dedini R, Behonick D, Werb Z, Miclau T, Marcucio R, Colnot C. Impaired remodeling phase of fracture repair in the absence of matrix metalloproteinase-2. Dis Model Mech. 2011 Mar; 4(2):203–211. [PubMed: 21135056]
51. Nyman JS, Lynch CC, Perrien DS, Thiolloy S, O'Quinn EC, Patil CA, Bi X, Pharr GM, Mahadevan-Jansen A, Mundy GR. Differential effects between the loss of MMP-2 and MMP-9 on structural and tissue-level properties of bone. J Bone Miner Res. 2011 Jun; 26(6):1252–1260. [PubMed: 21611966]
52. Noda M, Camilliere JJ. In vivo stimulation of bone formation by transforming growth factor-beta. Endocrinology. 1989 Jun; 124(6):2991–2994. [PubMed: 2721454]
53. Filvaroff E, Erlebacher A, Ye J, Gitelman SE, Lotz J, Heillman M, Derynck R. Inhibition of TGF-beta receptor signaling in osteoblasts leads to decreased bone remodeling and increased trabecular bone mass. Development. 1999 Oct; 126(19):4267–4279. [PubMed: 10477295]
54. Balooch G, Balooch M, Nalla RK, Schilling S, Filvaroff EH, Marshall GW, Marshall SJ, Ritchie RO, Derynck R, Alliston T. TGF-beta regulates the mechanical properties and composition of bone matrix. Proc Natl Acad Sci U S A. 2005 Dec 27; 102(52):18813–18818. [PubMed: 16354837]
55. Mohammad KS, Chen CG, Balooch G, Stebbins E, McKenna CR, Davis H, Niewolna M, Peng XH, Nguyen DH, Ionova-Martin SS, Bracey JW, Hogue WR, Wong DH, Ritchie RO, Suva LJ, Derynck R, Guise TA, Alliston T. Pharmacologic inhibition of the TGF-beta type I receptor kinase has anabolic and anti-catabolic effects on bone. PLoS One. 2009; 4(4):e5275. [PubMed: 19357790]
56. Edwards JR, Nyman JS, Lwin ST, Moore MM, Esparza J, O'Quinn EC, Hart AJ, Biswas S, Patil CA, Lonning S, Mahadevan-Jansen A, Mundy GR. Inhibition of TGF-beta signaling by 1D11 antibody treatment increases bone mass and quality in vivo. J Bone Miner Res. 2010 Nov; 25(11): 2419–2416. [PubMed: 20499365]
57. Geiser AG, Zeng QQ, Sato M, Helvering LM, Hirano T, Turner CH. Decreased bone mass and bone elasticity in mice lacking the transforming growth factor-beta1 gene. Bone. 1998 Aug; 23(2): 87–93. [PubMed: 9701466]
58. Atti E, Gomez S, Wahl SM, Mendelsohn R, Paschalis E, Boskey AL. Effects of transforming growth factor-beta deficiency on bone development: a Fourier transform-infrared imaging analysis. Bone. 2002 Dec; 31(6):675–684. [PubMed: 12531561]
59. Avivi E, Arzi H, Paz L, Caspi I, Chechik A. Skeletal manifestations of Marfan syndrome. Isr Med Assoc J. 2008 Mar; 10(3):186–188. [PubMed: 18494229]
60. Birch JG, Herring JA. Spinal deformity in Marfan syndrome. J Pediatr Orthop. 1987 Sep-Oct;7(5): 546–552. [PubMed: 3624465]
61. Jones KB, Erkula G, Sponseller PD, Dormans JP. Spine deformity correction in Marfan syndrome. Spine (Phila Pa 1986). 2002 Sep 15; 27(18):2003–2012.
62. Ehnert S, Baur J, Schmitt A, Neumaier M, Lucke M, Dooley S, Vester H, Wildemann B, Stockle U, Nussler AK. TGF-beta1 as possible link between loss of bone mineral density and chronic inflammation. PloS One. 2010; 5(11):e14073. [PubMed: 21124921]
63. Yang FC, Chen S, Clegg T, Li X, Morgan T, Estwick SA, Yuan J, Khalaf W, Burgin S, Travers J, Parada LF, Ingram DA, Clapp DW. Nf1 +/− mast cells induce neurofibroma like phenotypes through secreted TGF-beta signaling. Hum Mol Genet. 2006 Aug 15; 15(16):2421–2437. [PubMed: 16835260]
64. Wang W, Nyman JS, Moss HE, Gutierrez G, Mundy GR, Yang X, Elefteriou F. Local low-dose lovastatin delivery improves the bone-healing defect caused by Nf1 loss of function in osteoblasts. J Bone Miner Res. 2010 Jul; 25(7):1658–1667. [PubMed: 20200958]
65. Munger JS, Huang X, Kawakatsu H, Griffiths MJ, Dalton SL, Wu J, Pittet JF, Kaminski N, Garat C, Matthay MA, Rifkin DB, Sheppard D. The integrin alpha v beta 6 binds and activates latent TGF beta 1: a mechanism for regulating pulmonary inflammation and fibrosis. Cell. 1999 Feb 5; 96(3):319–328. [PubMed: 10025398]

66. Schultz-Cherry S, Murphy-Ullrich JE. Thrombospondin causes activation of latent transforming growth factor-beta secreted by endothelial cells by a novel mechanism. J Cell Biol. 1993 Aug; 122(4):923–932. [PubMed: 8349738]

67. Yu Q, Stamenkovic I. Cell surface-localized matrix metalloprotei-nase-9 proteolytically activates TGF-beta and promotes tumor invasion and angiogenesis. Genes Dev. 2000 Jan 15; 14(2):163–176. [PubMed: 10652271]

68. Kolanczyk M, Kossler N, Kuhnisch J, Lavitas L, Stricker S, Wilkening U, Manjubala I, Fratzl P, Sporle R, Herrmann BG, Parada LF, Kornak U, Mundlos S. Multiple roles for neurofibromin in skeletal development and growth. Hum Mol Genet. 2007 Apr 15; 16(8):874–886. [PubMed: 17317783]

69. Schindeler A, Morse A, Harry L, Godfrey C, Mikulec K, McDonald M, Gasser JA, Little DG. Models of tibial fracture healing in normal and Nf1-deficient mice. J Orthop Res. 2008 Aug; 26(8):1053–1060. [PubMed: 18383150]

70. Wang W, Nyman JS, Ono K, Stevenson DA, Yang X, Elefteriou F. Mice lacking Nf1 in osteochondroprogenitor cells display skeletal dysplasia similar to patients with neurofibromatosis type I. Hum Mol Genet. 2011 Oct 15; 20(20):3910–3924. [PubMed: 21757497]

71. Heervä E, Peltonen S, Svedström E, Aro HT, Väänänen K, Peltonen J. Osteoclasts derived from patients with neurofibromatosis 1 (NF1) display insensitivity to bisphosphonates in vitro. Bone. 2012 Mar; 50(3):798–803. [PubMed: 22226973]

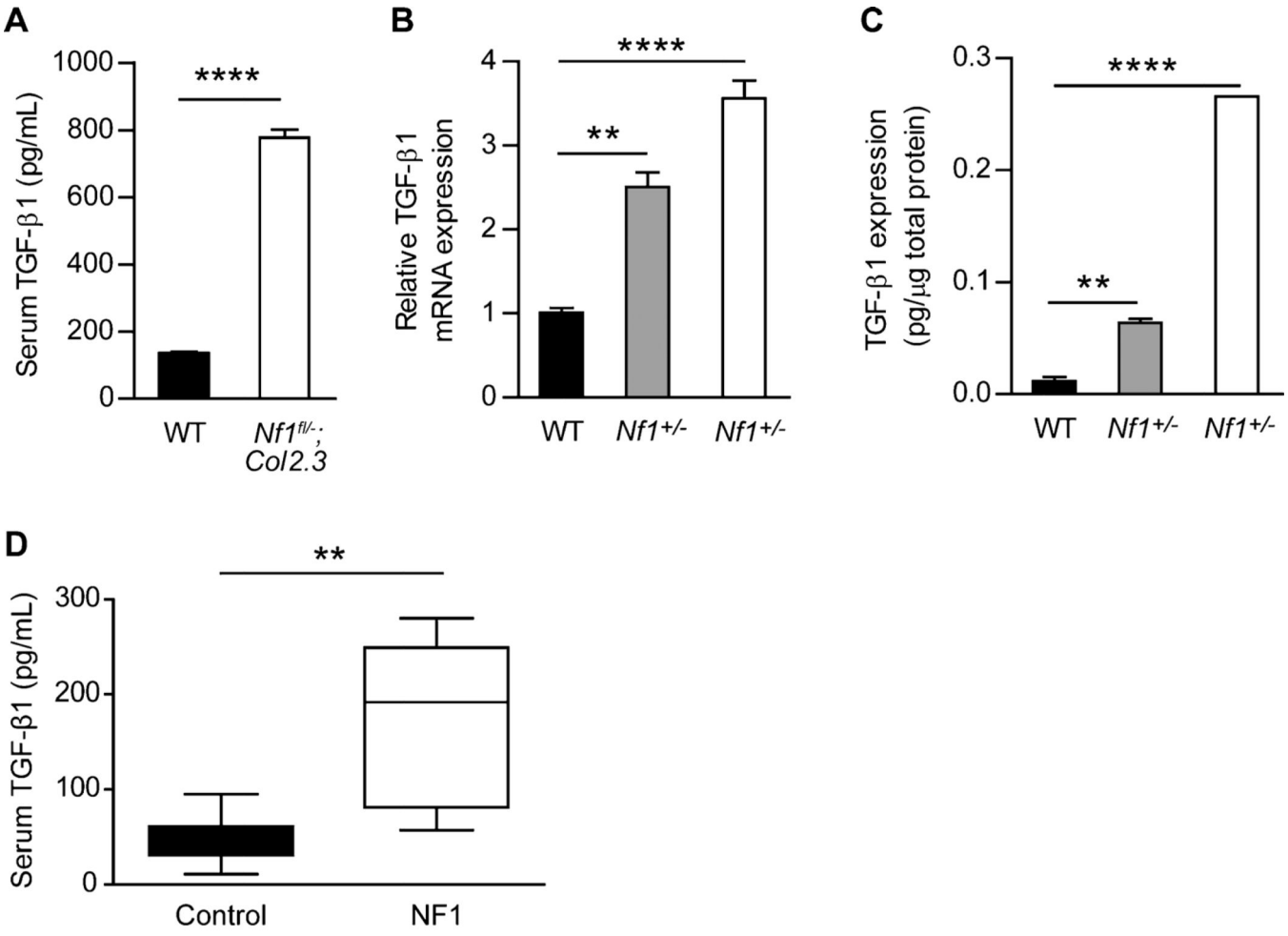

Fig. 1.

Nf1 gene dose regulates TGF-β1 production by osteoblasts. (*A*) Serum TGF-β1 levels were measured by ELISA in WT and $Nf1^{flox/-}$;*Col2.3Cre* mice. $n = 4$ mice per group. ****$p <$ 0.0001. (*B*) TGF-β1 mRNA expression in WT, $Nf1^{+/-}$, $Nf1^{-/-}$ osteoblast progenitors was examined by quantitative PCR. $n = 3$ technical replicates. The experiment was repeated twice with similar results using independent cell lines. **$p < 0.01$, ****$p < 0.0001$. (*C*) Protein extracts were examined by ELISA to determine TGF-β1 protein expression. $n = 3$ technical replicates. The assay was repeated twice with similar results using independent cell lines. **$p < 0.01$, ****$p < 0.0001$. (*D*) Serum TGF-β1 levels were measured by ELISA in human NF1 patients and healthy controls. $n = 7$ samples per group. **$p < 0.01$.

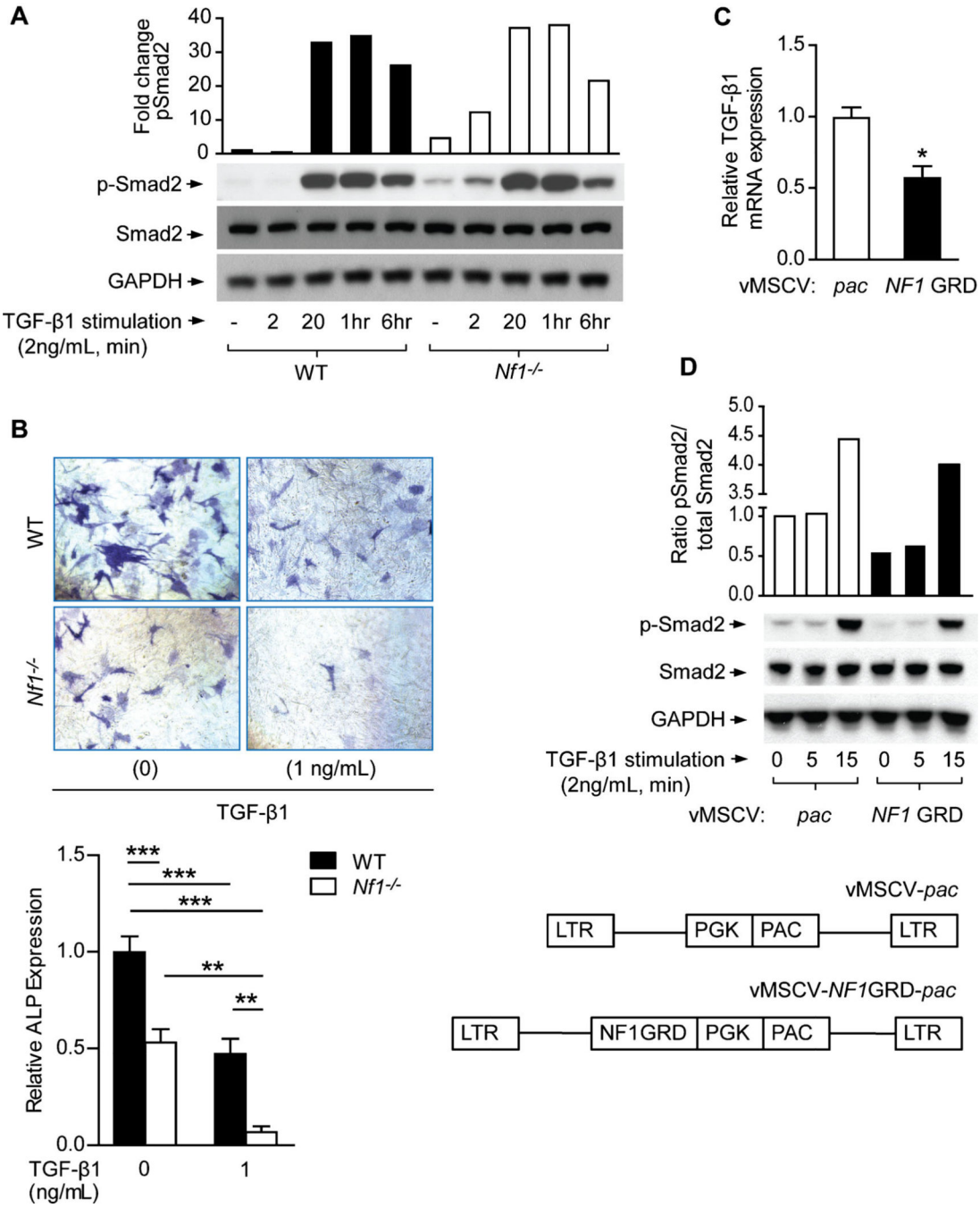

Fig. 2.

Nf1-deficient MSCs exhibit hyperactivation of the Smad pathway and impaired osteoblast differentiation in response to TGF-β1. (*A*) p-Smad2, Smad2, and GAPDH levels were detected by Western blot in MSCs stimulated with TGF-β1. The quantitative fold change in p-Smad2 was determined relative to the loading control, as shown in the bar graph. The experiment was repeated on three independent occasions with similar results. (*B*) MSCs were cultured in osteogenic differentiation medium supplemented with TGF-β1. Representative photomicrographs (top panel) show alkaline phosphatase (ALP)-positive

osteoblasts (magnification × 200). ALP expression was quantified and normalized to the WT control as shown (bottom panel). $n = 3$ technical replicates. The assay was repeated twice with similar results using independent cell lines. $^{**}p < 0.01$, $^{***}p < 0.001$. (*C*) TGF-β1 mRNA expression was measured in *Nf1*$^{-/-}$ MSCs following retroviral transduction with control vector (MSCV-pac) versus the functional, full-length *NF1* GRD construct. $n = 3$ technical replicates. The experiment was repeated on three independent occasions with similar results. $^{*}p < 0.05$. (*D*) p-Smad2, Smad2, and GAPDH levels were detected by Western blot in MSCs stimulated with TGF-β1 following transduction with either MSCV-pac or MSCV-*NF1* GRD retroviral vectors. The quantitative fold change in p-Smad2 was determined relative to the level of total Smad2 protein, as shown in the bar graph.

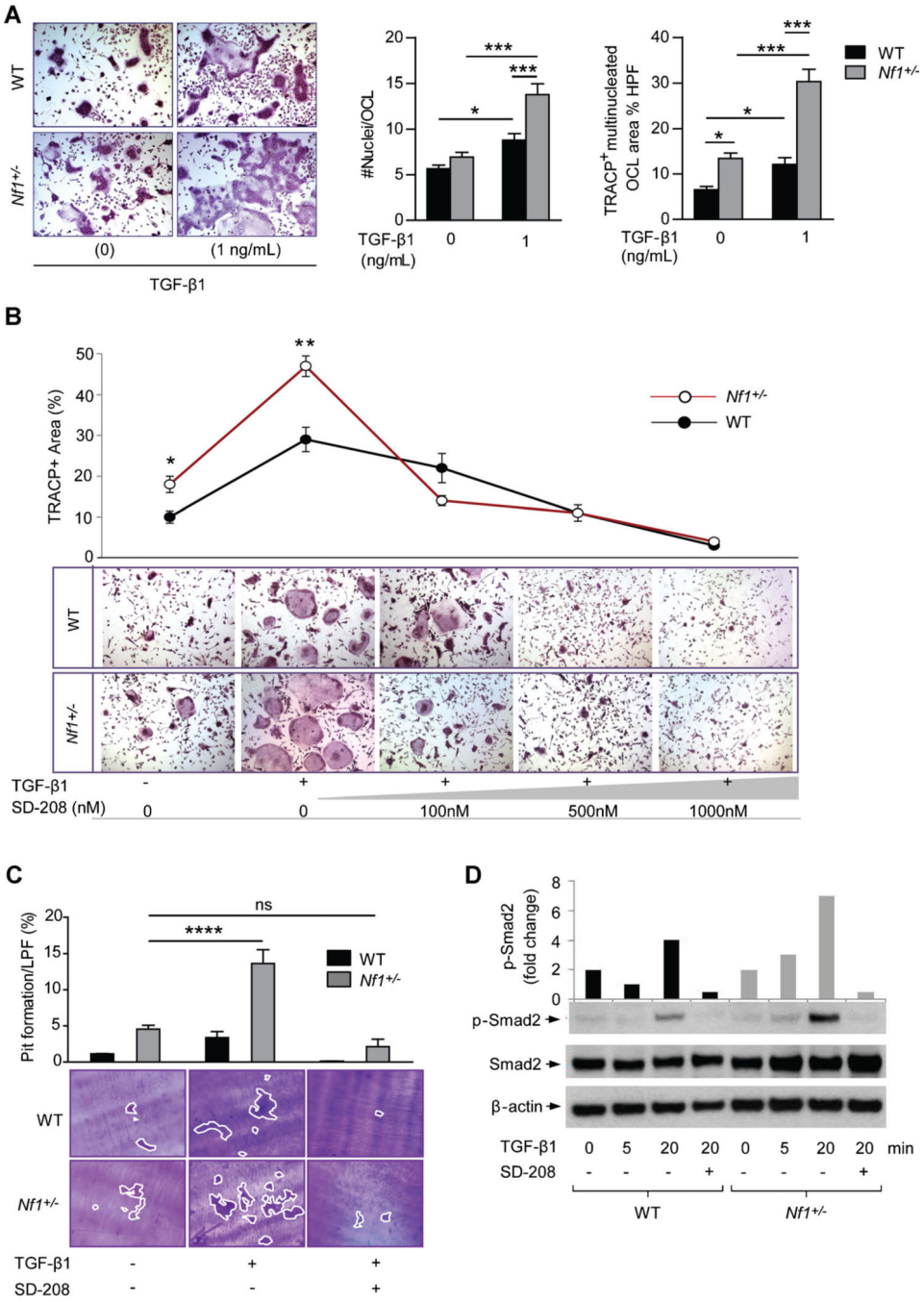

Fig. 3.

TGF-β1 potentiates *Nf1* haploinsufficient osteoclast gain-in-functions, which are accompanied by increased activation of the Smad pathway. (*A*) Osteoclast formation from BMMNCs was induced by M-CSF and RANKL, in the presence or absence of TGF-β1 (1 ng/mL). Representative photomicrographs show multinucleated osteoclasts (magnification ×200) following TRACP staining. Bar graphs represent the mean number of nuclei per osteoclast and the area of TRACP-positive, multinucleated osteoclasts per high power field (HPF), quantified using ImageJ software. n = 4 biological replicates. The experiment was

repeated three times with similar results. *$p < 0.05$, **$p < 0.001$. (*B*) Osteoclast formation following TGF-β1 stimulation and increasing doses of SD-208. $n = 3$ biological replicates. *$p < 0.05$, **$p < 0.01$ comparing $Nf1^{+/-}$ versus WT. (*C*) Osteoclast bone resorption on dentine slices. Representative photomicrographs show resorptive "pits" (magnification × 100). "Pit" area was quantified as shown by the bar graph above. $n = 3$ biological replicates. ***$p < 0.0001$. (*D*) Phosphorylated Smad2 (p-Smad2), total Smad2, and β-actin were measured by Western blot in preosteoclasts stimulated with TGF-β1 (1 ng/mL) in the presence or absence of SD-208 (100 nM). The bar graph shows the fold change in p-Smad2 relative to the loading control. The assay was repeated on two independent occasions with similar results.

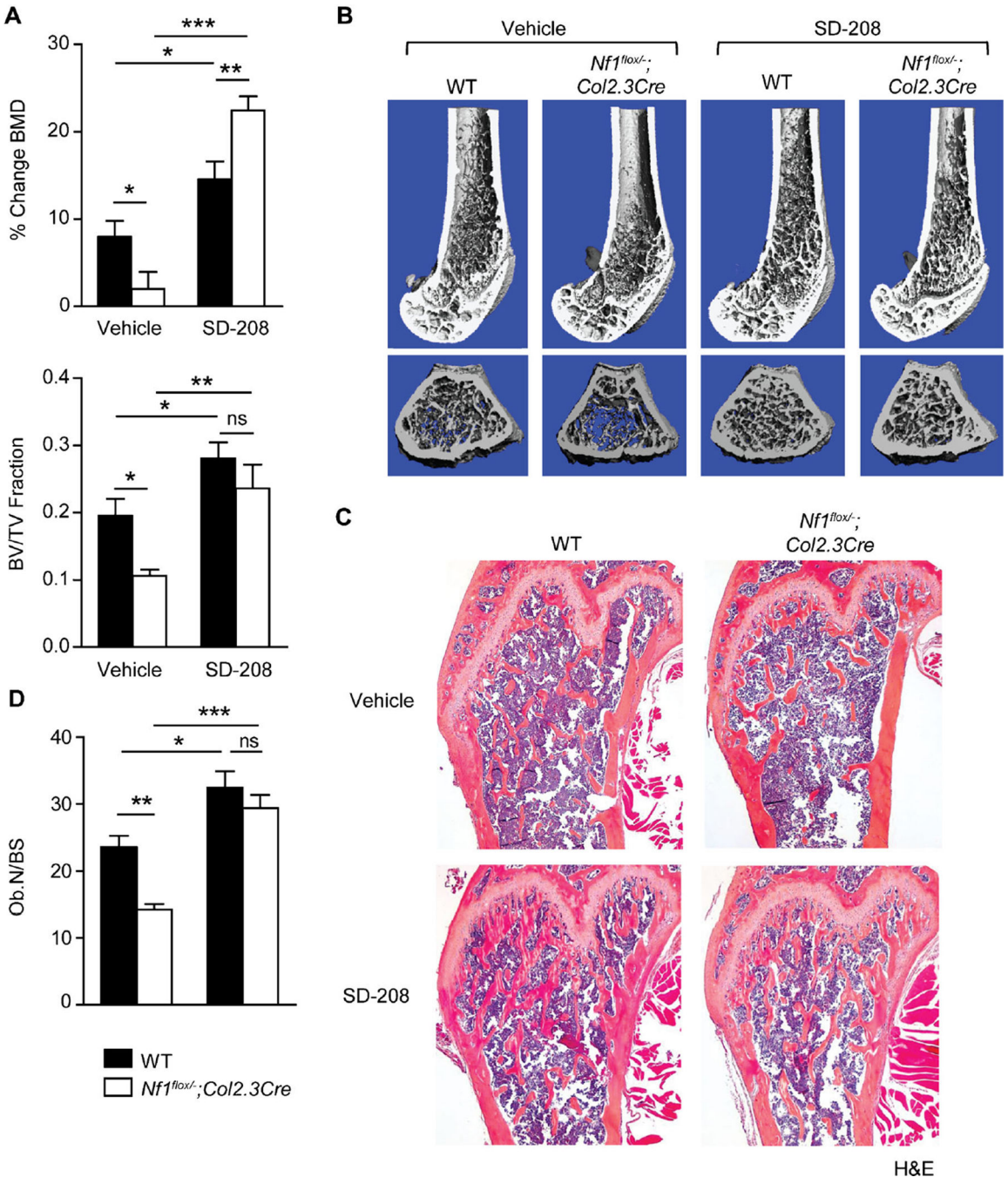

Fig. 4.

TβRI inhibition restores bone mass in *Nf1*$^{flox/-}$*;Col2.3Cre* mice. (*A*) (Top) The percentage change in BMD of the distal femur was determined by pDXA before and after 4 weeks of treatment with vehicle or SD-208 (60mg/kg/d). $n = 7$ to 12 mice per group. *$p < 0.05$, **$p < 0.01$, ***$p < 0.001$. (Bottom) Trabecular bone volume fraction (BV/TV) was quantified by μCT. $n = 7$ to 12 mice per group. *$p < 0.05$, **$p < 0.01$. (*B*) Representative μCT reconstructed femora in longitudinal (top) and transverse (bottom) cross-sections after 4 weeks treatment with vehicle or SD-208 treatment. (*C*) Representative longitudinal sections

of H&E stained femora, ×25 magnification. (*D*) The osteoblast number per millimeter of bone surface was quantified by manually counting osteoblasts on H&E-stained sections (×200 magnification). $n = 7$ to 12 mice per group. *$p < 0.05$, **$p < 0.01$, ***$p < 0.001$.

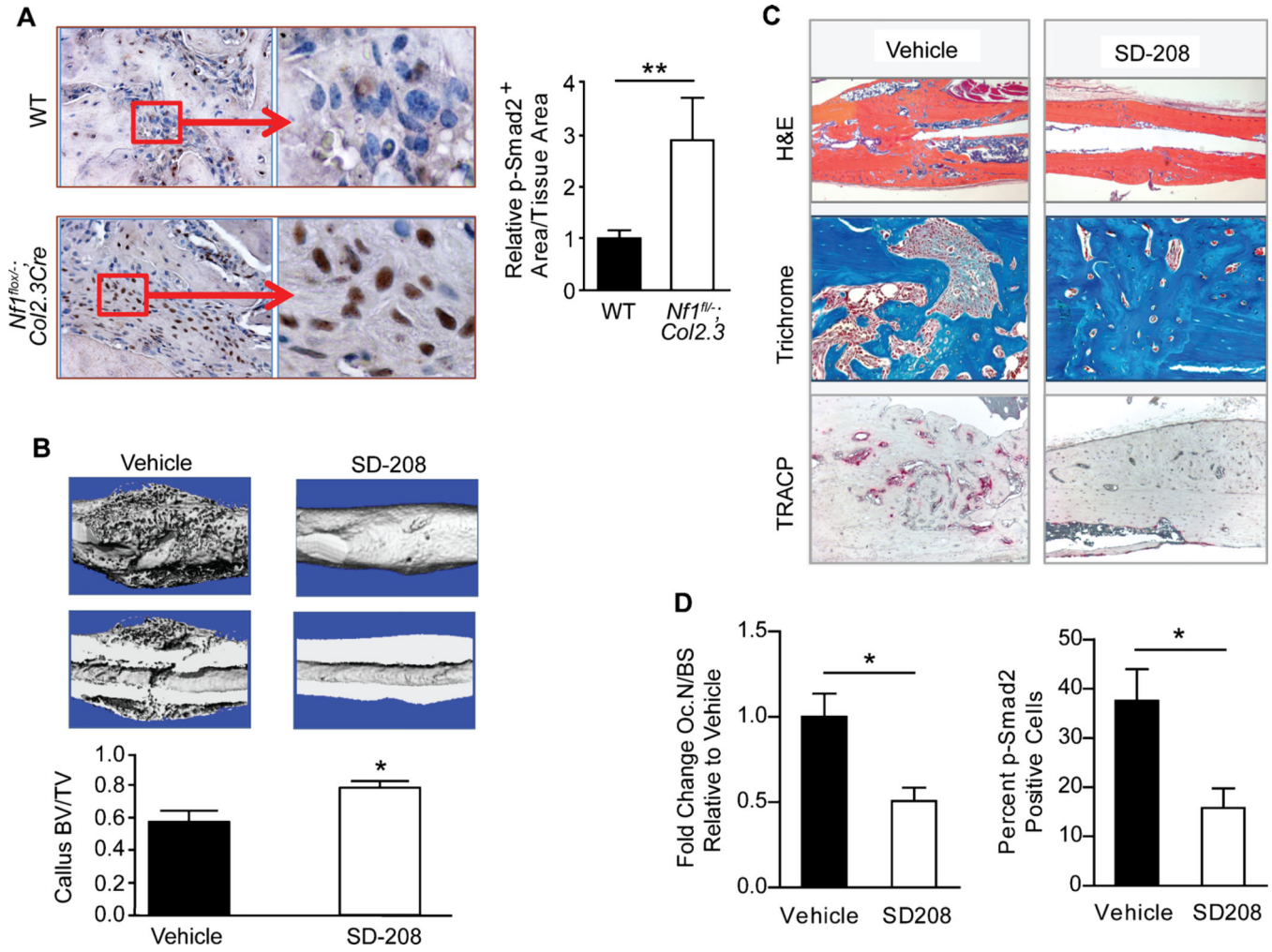

Fig. 5.

TβRI inhibition prevents tibial fracture nonunion in *Nf1$^{flox/-}$;Col2.3Cre* mice. (*A*) Immunohistochemical staining for p-Smad2 in fracture calluses of WT and *Nf1$^{flox/-}$;Col2.3Cre* mice. The p-Smad2–positive staining area was normalized to the tissue area and compared between genotypes. $n = 6$ mice per group. $^{**}p < 0.01$. (*B*) (Top) Representative μCT reconstructed whole callus and longitudinal cross-sections from *Nf1$^{flox/-}$;Col2.3Cre* mice treated with either vehicle or SD-208 for 4 weeks following tibial fracture. (Bottom) Callus bone volume fraction (BV/TV) was quantified by μCT as shown in the bar graph. $n = 6$ to 8 mice per group. $^{*}p < 0.05$. (*C*) Representative tibial fractures in longitudinal cross-sections stained with H&E (x25 magnification), trichrome (x100 magnification), and TRACP (x50 magnification). (*D*) (Left) The fold change in osteoclast number (Oc.N) per millimeter of bone surface (BS) in SD-208–treated *Nf1$^{flox/-}$;Col2.3Cre* mice relative to the vehicle-treated cohort was determined by manually counting multinucleated TRACP-positive cells. $n = 6$ mice per group. $^{*}p < 0.05$. (Right) Tibial fracture sections were immunostained for p-Smad2. The number of p-Smad2–positive cells was quantified as a percentage of the total cells per high power field. $n = 5$ to 6 mice per group. $^{*}p < 0.05$.

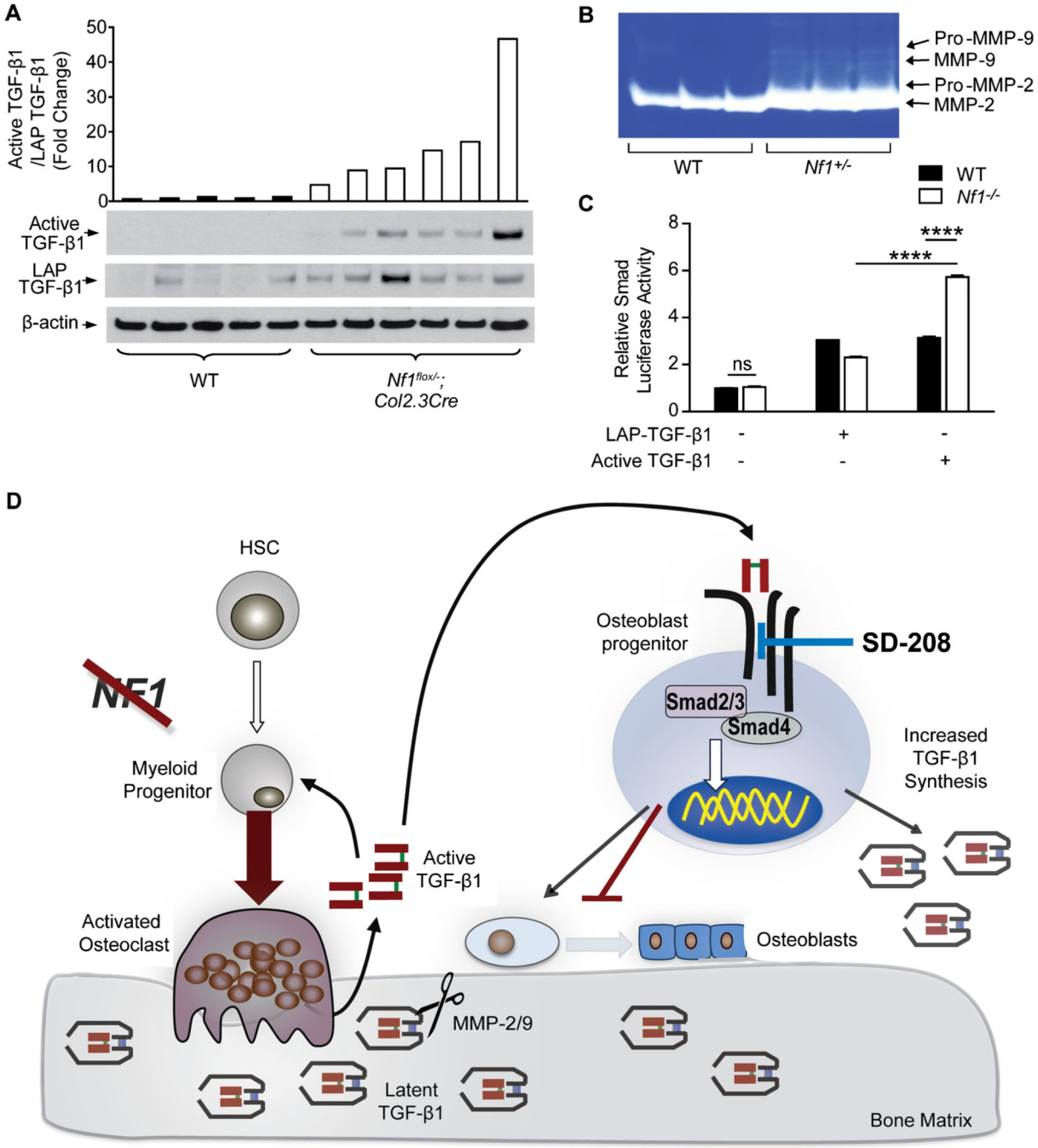

Fig. 6.

Hypersecretion of MMP-2/9 promotes excessive latent TGF-β1 activation. (*A*) Active TGF-β1, latency associated peptide (LAP)-bound TGF-β1, and β-actin were detected by Western blot in protein extracts from the fracture site of *Nf1*$^{flox/-}$;*Col2.3Cre* mice with tibial fracture nonunion and WT controls. The bar graph represents the fold change in the active TGF-β1/LAP-TGF-β1 ratio. $n = 5$ to 6 mice per group. (*B*) Activity levels of MMP-2/9 were measured in WT and *Nf1*$^{+/-}$ myeloid cell conditioned medium by zymography. $n = 3$ biological replicates. (*C*) Osteoprogenitors transfected with a Smad luciferase reporter were

stimulated with recombinant, active TGF-β1 (1 ng/mL) and latent, LAP-TGF-β1 (100 ng/mL) for 18 hours. $n = 3$ technical replicates. The experiment was repeated on two independent occasions with similar results. *$p < 0.05$, **< 0.01. (*D*) Working model of NF1 skeletal defects mediated by a pathological cycle of increased TGF-β1 synthesis, activation, and Smad signaling.